

Adaptive Pseudo-Label Refinement by Negative Ensemble Learning for Source-Free Unsupervised Domain Adaptation

Waqar Ahmed^{1,2}, Pietro Morerio^{1,3} and Vittorio Murino^{1,3,4}

¹Pattern Analysis & Computer Vision (PAVIS), Istituto Italiano di Tecnologia, Genova, Italy

²Dipartimento di Ingegneria Navale, Elettrica, Elettronica e delle Telecomunicazioni, University of Genova, Italy

³Ireland Research Center, Huawei Technologies Co. Ltd., Dublin, Ireland

⁴Dipartimento di Informatica, University of Verona, Italy

{waqar.ahmed, pietro.morerio, vittorio.murino}@iit.it

Abstract

The majority of existing Unsupervised Domain Adaptation (UDA) methods presumes source and target domain data to be simultaneously available during training. Such an assumption may not hold in practice, as source data is often inaccessible (e.g., due to privacy reasons). On the contrary, a pre-trained source model is always considered to be available, even though performing poorly on target due to the well-known domain shift problem. This translates into a significant amount of misclassifications, which can be interpreted as structured noise affecting the inferred target pseudo-labels. In this work, we cast UDA as a pseudo-label refinery problem in the challenging source-free scenario. We propose a unified method to tackle adaptive noise filtering and pseudo-label refinement. A novel Negative Ensemble Learning technique is devised to specifically address noise in pseudo-labels, by enhancing diversity in ensemble members with different stochastic (i) input augmentation and (ii) feedback. In particular, the latter is achieved by leveraging the novel concept of Disjoint Residual Labels, which allow diverse information to be fed to the different members. A single target model is eventually trained with the refined pseudo-labels, which leads to a robust performance on the target domain. Extensive experiments show that the proposed method, named Adaptive Pseudo-Label Refinement, achieves state-of-the-art performance on major UDA benchmarks, such as Digit5, PACS, Visda-C, and DomainNet, without using source data at all.

1. Introduction

Deep Convolutional Neural Networks (CNNs) have shown remarkable achievements in a variety of tasks [8]. However, to perform well, training and testing data are as-

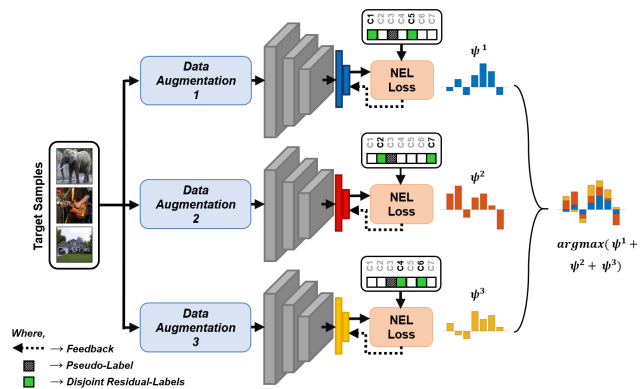


Figure 1: Illustration of the proposed unified technique for adaptive noise filtering and progressive pseudo-label refinement (AdaPLR). After inferring target pseudo-labels using the source model, each ensemble member is trained using a batch of target samples with different stochastic (i) input augmentation and (ii) feedback, by leveraging *Disjoint residual labels* and *Negative Ensemble Learning* (NEL) loss.

sumed to be drawn from the same distribution. This is unrealistic when the system needs to be deployed in real-world scenarios. Consequently, a model trained on some source domain often fails to generalize well on a related but different target domain, due to the well-known *domain shift* [40] problem. Since annotating data from every possible domain is expensive and sometimes even impossible, Unsupervised Domain Adaptation (UDA) methods seek to address such a problem by minimizing discrepancy across the domains or trying to learn domain-invariant feature embeddings, without accessing target label information. Most UDA works focus on the single-source/single-target scenario, regardless of the fact that data may belong to multiple source or target distributions, e.g., images taken in different environments or obtained from the web (such as sketches, photos, etc.).

Our framework naturally allows to cope with any number of source and target domains, unlike previous literature.

Several research efforts have been devoted to developing UDA methods by either enforcing class-level feature distribution alignment [5, 7], matching moments [33, 4], applying domain-specific batch normalization [3], or adopting domain adversarial learning [39]. However, all of these methods require joint access to both (labeled) source and (unlabeled) target data during training, making them unsuitable for scenarios where source data is inaccessible during the adaptation stage, or when source and target data are not available at the same time. Further, such solutions are also not viable when target data is provided incrementally at different times or if the source/target datasets are very large.

In this paper, to get rid of such restrictive assumptions, we propose to address UDA from a novel perspective, *i.e.*, by casting it as a pseudo-label refinement problem in a source data-free scenario. In particular, our proposed framework assumes a model pre-trained on the source domain to infer *pseudo-labels* of unlabeled target samples. This results in a significant amount of incorrect pseudo-labels, which we interpret as *shift-noise* [29] affecting the ground-truth target data labels. To clean such labels, we propose Negative Ensemble Learning, a novel pipeline where each member of an ensemble is trained using a batch of target samples with different stochastic input augmentation together with the novel concept of disjoint-feedback using *Disjoint Residual Labels*.

The intuition behind using an ensemble is that in the case of wrong pseudo-labels at least $N_e - 1$ members out of N_e can receive the correct information. This is made possible by the fact that in Negative Learning only the complement (or residual) of the original label is used as feedback for the networks. Further, stochastically sampled disjoint subsets of residual labels force the ensemble members to learn different concepts, which is known to be beneficial in ensemble learning to reach a strong consensus. A strong consensus also achieves a higher probability on clean pseudo-labels, allowing us to introduce a novel *fully adaptive* noise filtering technique which allows refining labels of the samples with low confidence (*i.e.*, noisy pseudo-labels) via re-assignment. Finally, a standard supervised learning procedure is used to train a *single* model on the target domain data with the refined pseudo-labels featuring high confidence only.

The proposed pipeline obtains significant noise reduction from the inferred pseudo-labels. With extensive experiments on benchmarks with diverse complexity and issues, we show that training on the target domain with refined pseudo-labels outperforms state-of-the-art UDA methods by a considerable margin. To summarise, the contributions of our work can be stated as follows.

- We are the first to cast the source-free UDA problem in the framework of label noise reduction. Further, we are

proposing a method that can cope with single-source, multi-source and multi-target UDA indifferently, unlike most of the former works.

- We propose a new, fully-adaptive method that dynamically filters out label noise and assign cleaner pseudo-labels to noisy target samples. To do so, we introduce Negative Ensemble Learning, a new strategy that enhances diversity among members, which improve noise resilience and leads to a stronger consensus.
- We validate our proposed method through detailed ablation analyses and extensive experiments on four well-known public benchmarks, demonstrating its superiority over state-of-the-art UDA methods (with a large margin of up to 21.8% for PACS benchmark).

The remainder of the paper is organized as follows. In Section 2, we discuss related works. Section 3 describes the proposed method to tackle source-free UDA. Section 4 illustrates the experimental setup and reports the obtained results. Finally, the conclusions are drawn in Section 5.

2. Related Work

Unsupervised Domain Adaptation. Most of the existing UDA methods focus on cross-domain feature *alignment*, either by employing sampling-based implicit alignment [19], locality preserving projection based subspace alignment [28], discriminative class-conditional alignment [7], features and prototype alignment using reliable samples [5], or a customized CNN with domain alignment layers and feature whitening [35]. Some other works propose feature distribution *matching* by approximating joint distribution [41], graph matching [9], moment matching [33], and higher-order moment matching of non-Gaussian distributions[4]. However, such methods assume co-existence of source and target data during training, making them unsuitable for more realistic scenarios where source data is inaccessible, *e.g.*, due to data-privacy issues.

Source-free UDA. Some recent works focus on the source-free UDA. For instance, [6] proposes a feature corruption and marginalization technique using few labeled source samples as representative examples, and [30] adapts the outputs from an off-the-shelf model to minimize label deficiency and distribution shift using some labeled target samples. An instance-level weighting method using negative classes is proposed in [22] which is highly dependent on procurement stage which requires the source data. Another approach leverages a pre-trained source model to update the target model progressively by generating target-style samples through conditional generative adversarial networks [29], also combined with clustering-based regularization [26]. Similarly, to improve UDA performance in person re-identification task, [15] proposes a pseudo-label cleaning process with on-line refined soft pseudo-labels.

Our proposed approach lies in this category and partially takes inspiration from the approaches developed for source-free UDA in [26, 29]. In both methods, a pre-trained source model is used to infer pseudo-labels of target data, and then exploit a target-style sample generator for adaptation. We instead tackle source-free UDA from a novel perspective, namely by progressively refining pseudo-labels exploiting the consensus of an ensemble network, without generating any (target-style) data.

Ensemble Learning Methods. Such methods exploit features extracted from multiple models (typically CNNs) through a diversity of projections on data, and bring forward the mutual consensus to achieve better performances than those obtained by any individual model [48]. A comprehensive review about ensemble methods is well presented in [12]. The concept of diversity contribution ability for classifier selection and weight adjustment is proposed in [46]. Also, multiple choice learning is employed in [14] to improve the accuracy of an ensemble of models.

We draw inspiration from the general idea proposed in these works, which agree in stressing that *diversity* among members is beneficial for ensemble robustness. We differentiate from them by introducing a novel way of inducing diversity in the members, *i.e.* we back-propagate different feedback to each member by leveraging the novel concept of Disjoint Residual Labels. This allows each member to learn something diverse and possibly complementary, leading to a stronger consensus and noise resilience.

Learning with Noisy Labels. Deep CNNs are capable of memorizing the entire data even when labels are noisy [21]. To overcome such overfitting over noisy samples, existing methods try to select a subset of possibly clean labels for training, *e.g.*, using two networks under a co-teaching framework [17], meta-learning based exemplar weight estimation [47], one-out filtering approach based on the local and global consistency algorithm [10], or Negative Learning (NL) as an indirect learning method [21].

However, these works only consider random noise from selective or uniform distribution which has a completely different structure from the domain-shift noise associated with the inferred pseudo-labels (see Section 3.1). Our work is inspired by [21] which presents a Negative Learning (NL) approach to clean samples with noisy labels. Nevertheless, [21] fails when the noise is not uniform, and the performance is actually affected by threshold sensitivity, which limit the generalization capability of the method across benchmarks. In contrast to a fixed threshold, our method features a fully *adaptive* procedure to progressively filter out the actual (structured) noise affecting target pseudo-labels under domain shift (*shift-noise* [29]): as the ensemble gets more and more confident in the clean examples during training, label reassignment becomes more rigorous, which prevents the network to overfit noisy samples.

3. The Method

In this section, we first review the background notions behind the employed techniques – Negative Learning and Ensemble Learning – highlighting their limitations along with the proposed advancements. Then, we illustrate the problem setup and detail the proposed AdaPLR method.

3.1. Background and Notation

Negative Learning (NL). It was proposed by [21] which refers to an indirect learning method that leverages inverse supervision. In short, the feedback given to a classifier does not follow the usual ”this is class c ” logic, but rather a ”this is *not* class \bar{c} ” scheme. The intuition is that, by sampling \bar{c} from the complement set of c , there are less chances of providing wrong feedback to the network in case the label c is incorrect.

In this paper, we schematize classical NL in the context of UDA for a C -class classification task as follows:

1. We use a source model to infer pseudo-labels for the whole target set \mathcal{D}_t . Such set of labels will be noisy.
2. For a given sample \mathbf{x} with inferred pseudo-label \tilde{y} , we train the network with a complementary label \bar{y} (randomly selected from $\{1, \dots, C\} \setminus \{\tilde{y}\}$) by *minimizing* the probability of \mathbf{x} belonging to \bar{y} .

Note that the the standard procedure would require *maximizing* the probability of \mathbf{x} belonging to \tilde{y} . In case of wrongly inferred pseudo-label $\tilde{y} \neq y_t$ (where y_t is the inaccessible actual target label) the network would undeniably be provided the wrong information. Instead, our schematized NL approach would reduce such probability to $\frac{1}{(C-1)}$.

Let our CNN architecture be composed of a feature extractor $\nu_\phi(\cdot)$, a classifier $\psi_\theta(\cdot)$, and a *softmax* $\sigma(\cdot)$, being ϕ and θ the related network parameters. The function $f : \mathcal{X} \rightarrow \mathbb{R}^C$, defined as $f(\mathbf{x}) = \sigma(\psi_\phi(\nu_\theta(\mathbf{x})))$ ¹, maps the input $\mathbf{x} \in \mathcal{X}$ to the C -dimensional vector of probabilities $\mathbf{p} \in \mathbb{R}^C$. Within a standard training procedure, namely Positive Learning (PL), the cross entropy loss function can be defined as:

$$\mathcal{L}_{PL}(\mathcal{D}_t) = -\mathbb{E}_{\mathbf{x}_t \sim \mathcal{D}_t} \sum_{c=1}^C \mathbb{1}_{[c=\tilde{y}]} \log(\mathbf{p}) \quad (1)$$

where $\mathbb{1}$ is an indicator function, \mathcal{D}_t represents the unlabeled target domain and $\mathbf{p} = f(\mathbf{x}_t)$. Clearly, Eq. (1) pushes the probability p for the given pseudo-label \tilde{y} towards $\mathbf{p}_{\tilde{y}} = 1$. On the contrary, NL aims at encouraging the probabilities of complementary labels \bar{y} to move away from 1, actually pushing them towards $\mathbf{p}_{\bar{y}} = 0$. The NL

¹Networks’ parameters θ and ϕ will be omitted for brevity from now on.

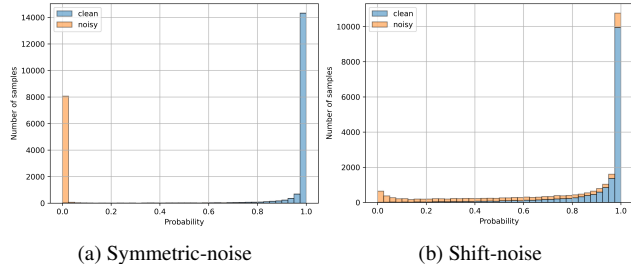


Figure 2: Histogram showing the noise-filtering performance of [21] on MNIST. In both cases, the amount of noise equals 32.9% (cf. SVHN→MNIST shift-noise in Table 1).

loss function would be so defined as:

$$\mathcal{L}_{NL}(\mathcal{D}_t) = -\mathbb{E}_{x_t \sim \mathcal{D}_t} \sum_{c=1}^C \mathbb{1}_{[c=\bar{y}]} \log(1 - p) \quad (2)$$

where \bar{y} is selected randomly from $\{1, \dots, C\} \setminus \{\tilde{y}\}$ at every training iteration. While Eq. (2) optimizes the output probability of the complementary label to be close to zero, the probability values of other classes are increased. In such a contest, the samples carrying clean \tilde{y} get higher confidence, whereas noisy ones struggle with scarcely confident scores, meeting the purpose of NL. Nevertheless, the fundamental limitation of naive NL [21] is that it is suitable for the noise showing a uniform distribution (*symmetric-noise*) only. As reported in Figure 2a, data samples with labels are assigned low confidence, resulting in effective noise separation.

Yet, a significant amount of noise is overfitted with high confidence by the network when we consider *shift-noise*, namely noise produced by inferring pseudo-labels on the target by using a model trained with the source (MNIST and SVHN, respectively, in the example of Figure 2b). Note that overfitting is not to be ascribed to the *amount* of noise, which was carefully balanced in the experiment, but rather to its *distribution* (for more details see the Appendix).

Ensemble Learning. It refers to concurrently training multiple networks of similar configuration on the same set of inputs. The idea is to create a set of experts trained in different ways, in order to produce predictions with low bias and high variance. Generally, the ensemble produces the final output as a weighted sum of all the experts' logits, *i.e.*, for a data sample \mathbf{x} , the final prediction can be defined as:

$$\mathbf{p}_e = \sigma\left(\sum_{k=1}^{N_e} \alpha^k \psi^k(\nu^k(\mathbf{x}))\right) \quad (3)$$

where N_e corresponds to the number of experts in the ensemble network and α^k is a set of weights that defines the contribution of each member. In this work we set $\alpha^k = 1, \forall k \in [1, N_e]$ and propose a novel Negative Ensemble Learning technique for learning with noisy labels that,

amplifies the diversity of the ensemble members by different stochastic (i) input augmentation, and (ii) feedback using Disjoint Residual Labels. The resulting strong consensus gives rise to the cleaner pseudo-labels, better than those obtained by any stand-alone network.

3.2. Adaptive Pseudo-Label Refinement (AdaPLR)

Problem Setup. The goal of UDA methods is to adapt a model pre-trained on a labelled source domain $\mathcal{D}_s = \{(\mathbf{x}_s^i, y_s^i)\}_{i=1}^{N_s}$ in order to generalize well on a different, yet related, unlabeled target domain $\mathcal{D}_t = \{\mathbf{x}_t^j\}_{j=1}^{N_t}$, where N_s and N_t denote the number of samples in the source and the target domain, respectively. In general, we assume working with $M_d + 1$ domains, including a target domain \mathcal{D}_t and source domains \mathcal{D}_s , where $s = \{1, \dots, M_d\}$. The main distinction between our approach and most standard UDA methods is that we do not use source data nor generate target-style data at any stage of the proposed method. Instead, we use only a pre-trained source model to infer pseudo-labels $\mathcal{P} = \{\tilde{y}^j\}_{j=1}^{N_t}$ on the target domain. Since this results in a significant amount of incorrect labels (due to domain shift [40]), we propose a way to progressively filter out noisy target samples from the clean ones, and carry out pseudo-label refinement to obtain cleaner \mathcal{P} .

Pseudo-Label Refinement. The prerequisite step for our proposed method refers to inferring pseudo-labels \mathcal{P} of unlabeled data samples of \mathcal{D}_t using f_s – a pre-trained model on the labeled samples from \mathcal{D}_s . Specifically, for *single-source* UDA, the model pre-trained on the chosen source is used to infer pseudo-labels of every target domain being considered. For *multi-source* UDA, we have two possibilities in which off-the-shelf pre-trained models can be used:

1) A single model pre-trained on the dataset of aggregated sources f_{agg} is used to infer \mathcal{P} , which is defined as:

$$\tilde{y}^j = \operatorname{argmax}(\psi_{agg}(\nu_{agg}(\mathbf{x}_t^j))) \quad \forall j \in \{1, \dots, N_t\}, \quad (4)$$

2) A set of M_d models, each pre-trained on one of the sources considered, f_1, \dots, f_{M_d} , are used to infer \mathcal{P} . The adopted strategy in this case is known as late-fusion, which is defined as,

$$\tilde{y}^j = \operatorname{argmax}\left(\sum_{s=1}^{M_d} \psi_s(\nu_s(\mathbf{x}_t^j))\right) \quad \forall j \in \{1, \dots, N_t\}, \quad (5)$$

In this study, we employ Eq. (4) as it represents a more realistic scenario in which a single available model is pre-trained on the maximum data at hand, *i.e.*, data aggregated from all possible sources. Later, for scalability, Eq. (5) can be used to leverage additional pre-trained source models.

Subsequently, the proposed AdaPLR method is applied. In particular, we obtain robust and cleaner pseudo-labels to refine \mathcal{P} using the moving average of N_a previous ensemble output predictions:

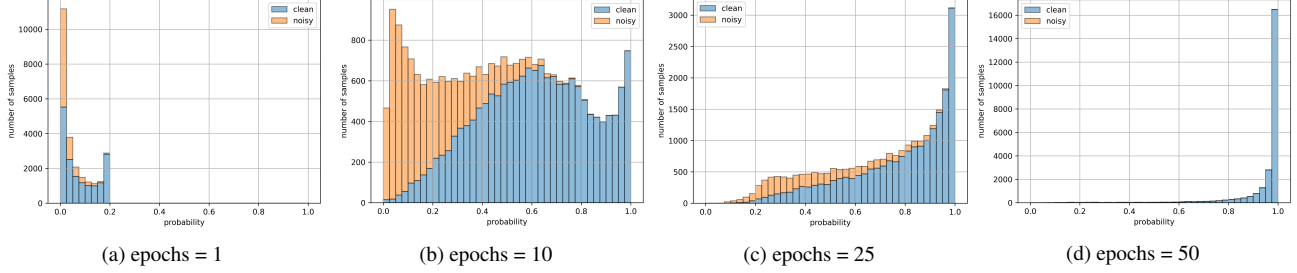


Figure 3: Prediction-confidence trend during training and pseudo-label refinement by our proposed AdaPLR method in case of SVHN→MNIST source-free UDA. Almost all samples are predicted with very low confidence at the beginning (a). As the network starts learning, noisy samples are segregated in a low confidence interval. Only if confidence is lower than γ (eq. 7), pseudo-labels are reassigned. Noise is thus progressively reduced (c-d). (Best viewed in color)

$$\mathbf{p} = \sigma\left(\frac{1}{N_a \cdot N_e} \sum_{l=1}^{N_a} \sum_{k=1}^{N_e} \psi_e^{k,l}(\nu_e^{k,l}(\mathbf{x}))\right) \quad (6)$$

where we set $N_a = 10$ for all the experiments in this study.² Now let us define \tilde{p} as the confidence of the pseudo-label \tilde{y} , namely the entry of the probability vector \mathbf{p} corresponding to \tilde{y} . We categorize the target samples with $\tilde{p} > \alpha$ as High Confidence Samples (HCS), and define the ratio of HCS over the total number of samples, as follows:

$$\gamma = \frac{\# \text{ of HCS}}{N_t} \quad (7)$$

During training, the pseudo-label of each sample \mathbf{x}_t^j is updated/retained according to the following condition:

$$\tilde{y}^j(n) = \begin{cases} \operatorname{argmax}(\mathbf{p}^j), & \text{if } \tilde{p}^j < \gamma \\ \tilde{y}^j(n-1), & \text{otherwise} \end{cases} \quad \forall j \quad (8)$$

where n denotes the epoch number. The intuition behind such reassignment rule can be drawn from the trend of the prediction confidence along training. As shown in Figure 3a and 3b, with the growing number of epochs, noisy samples remain towards low confidence regime and clean samples obtain high confidence progressively. In Figure 3b, the ratio of HCS (with $\alpha = 0.9$) gives $\gamma \approx 0.15$ that corresponds to a confidence region $[0, \gamma] = [0, 0.15]$ in which the noisy samples are prevalent, hence they are the best candidates to be subjected to label reassignment. Consequently, pseudo-label refinement is achieved progressively during training in an adaptive manner (see Figure 3c and 3d, where total noise is progressively reduced). We ablate to find optimal value of α in Section 4.2.

3.3. Negative Ensemble learning

Working with an ensemble allows us to make a smart use of more than one complementary label, *i.e.*, *Residual Labels*

²We anticipate that this is a non sensitive parameter, it has not a relevant effect on the performance as long as $N_a \geq 5$.

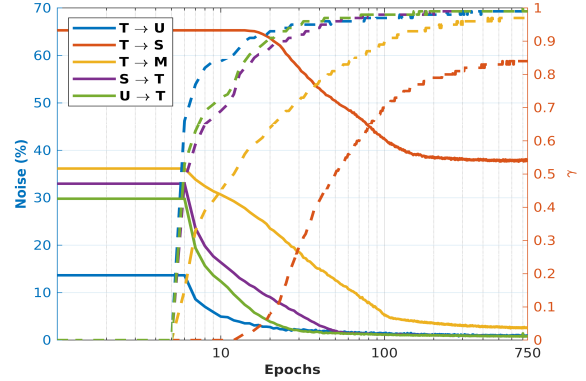


Figure 4: Correlation between adaptiveness of γ threshold (right y -axis, dashed profiles) and progressive noise reduction (left y -axis, solid profiles) achieved by AdaPLR during training for various amount of noise. Legend: **T**: MNIST, **S**: SVHN, **U**: USPS, and **M**: MNIST-M.

(*RL*), for each sample. So, let us consider the case we pick N_{RL} Residual Labels at once: this influences the training process in three ways: (a) The likelihood of the actual-label y_t being randomly picked as one of the complementary labels is now $\frac{N_{RL}}{C-1}$, which is bad. (b) In case $y_t \cap RL = \emptyset$, the training is accelerated by the stronger feedback provided by the multiple contributions of RLs, which is good. (c) In case $y_t \cap RL \neq \emptyset$, instead of providing entirely wrong feedback using Eq. 2, the impact of wrong feedback is mitigated by a factor of $\frac{N_{RL}-1}{N_{RL}}$, and this is again good. In fact, gradients will follow a mean direction according to the new Negative Ensemble Learning (NEL) loss that we define as:

$$\mathcal{L}_{NEL}(\mathcal{D}_t) = -\mathbb{E}_{\mathbf{x}_t \sim \mathcal{D}_t} \frac{1}{N_{RL}} \sum_{c=1}^C \mathbb{1}_{[c \in RL]} \log(1 - p_c) \quad (9)$$

Although (b) & (c) above are essential advantages of using multiple RL, (a) is a downside. Therefore, we ablate on the different values of N_{RL} in Section 4.2.

Disjoint Residual Labels. We further extend the idea of RL by introducing the concept of Disjoint Residual Labels (DRL) which is especially suited for ensembles, ($N_e > 1$).

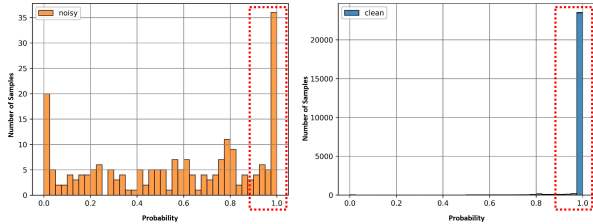


Figure 5: Distribution of remaining noise in refined pseudo-labels after SVHN→MNIST UDA. The highlighted bars represent the set of samples with confidence greater than $\alpha = 0.9$.

Each ensemble member can in fact be trained using Eq. 9, but with a completely *disjoint* stochastic subset of residual labels. Not only this allows each member to receive a different feedback (thus enhancing the ensemble’s diversity) but also restricts the possibility of receiving wrong feedback to one member only.

Stochastic Augmentations. The second strategy to induce additional diversity in ensemble members consists in feeding each member with the same batch of input images with different stochastic data augmentation. We consider several stochastic data augmentation strategies including the composition of (i) spatial/geometric transformation via random cropping (with uniform area = 0.08 to 1.0 and aspect-ratio = $\frac{3}{4}$ to $\frac{4}{3}$) followed by resizing to the original size, (ii) affine transformation followed by Gaussian blur, and (iii) color distortion. We found that composition of different stochastic data augmentation is crucial to avoid noise overfitting and extend diversity in the ensemble network (See Section 4.2).

All these ingredients concur in solving the shortcomings highlighted in Fig. 2. AdaPLR is in fact capable of filtering out different amounts of noise in an adaptive manner while refining pseudo-labels progressively. Trends with respect to right y -axis in Figure 4 show the capability of the threshold γ to adapt to different single-source UDA cases, while trends with respect to left y -axis show the corresponding noise reduction. In particular, it is worth noting that no pseudo-label refinement is applied during the first few epochs, until the ensemble gets a mature state of generalization capability.

After a certain number of training epochs, the pseudo-label refinement process stalls down to an insignificant noise reduction rate (see Figure 4). Therefore, instead of pushing AdaPLR more for several epochs to achieve further small reduction, we apply standard supervised learning only using high confidence samples determined by α . This is done using only one model (the final target model) for a fair comparison with state-of-the-art methods. As shown in Figure 5, the remaining noise is distributed over the entire probability spectrum, whereas the majority of the clean samples are predicted with high confidence (red box). Therefore,

only a small fraction of noisy samples affects training.

4. Experiments

4.1. Datasets and implementation details

We consider the image classification task to comprehensively evaluate the proposed AdaPLR method on major UDA benchmarks including Digit5 (MNIST [23], SVHN [31], USPS [11], MNIST-M [13], and Synthetic-Digits [13]), PACS [25], VisDA-C [34], and DomainNet [33]. For all the benchmarks, we use batch-size = 32, $\alpha = 0.9$ and Adam as the optimizer with a weight decay of $5e^{-4}$. The base learning rate is set to $1e^{-4}$ and the feature extractors are optimized with a learning rate of $1e^{-5}$. The feature extractor of ensemble members are initialized with a pre-trained source model. For single-source and multi-target UDA, we consider one pre-trained source model to adapt on every target domain. For multi-source UDA, each domain is selected as the target domain while the rest of the domains are treated as aggregated source (according to Eq. 4).

Digit5 refers to a set of digit benchmarks. In this paper, following [33], we sample a subset of 25000 images from the training and 9000 images from the testing set for MNIST, MNIST-M, SVHN, and Synthetic-Digits. Since USPS contain a total of 9298 images, we use standard train-test splits. To keep comparable image resolution, we resize all images to 32×32 and a naive 3-layer CNN is used as ensemble members. For single-source and multi-source UDA, label refinement takes 750 and 300 epochs, respectively, whereas the final target model is trained for 200 epochs.

PACS contains 4 domains, namely (*Art-Painting, Cartoon, Photo, and Sketch*). There are only 9991 images of 227×227 resolution from 7 object categories that accommodates a large domain shift due to the different image style depictions. We use ResNet-18 as ensemble members. For single-source, multi-target and multi-source UDA, label refinement takes 200, 200 and 100 epochs, respectively, whereas the final target model is trained for 200 epochs.

Visda-C is a challenging large-scale benchmark attempting to bridge the significant synthetic-to-real domain gap across 12 object categories. We follow standard protocol in which the source domain (training split) contains 152K synthetic images and the target domain (testing split) contains 72K real images. We resize all images to 256×256 resolution and use ResNet-101 as ensemble members. Label refinement takes 150 epochs and just 25 epochs were found to be enough for training the final target model.

DomainNet is by far the largest UDA benchmark with 6 domains, 600K images and 345 categories. We resize all images to 256×256 and use ResNet-101 as ensemble members. It was mainly developed for multi-source UDA task for which our proposed label refinement takes 100 epochs for *Infograph* and *Quickdraw* domain, while 40 epoch were

Source	Single-Source UDA						Multi-Source UDA						
	<i>T</i>	<i>T</i>	<i>T</i>	<i>S</i>	<i>U</i>	Avg.	<i>M,S</i>	<i>T,S</i>	<i>T,M</i>	<i>T,M</i>	<i>T,M</i>	Avg.	
	<i>U</i>	<i>S</i>	<i>M</i>	<i>T</i>	<i>T</i>		<i>D,U</i>	<i>D,U</i>	<i>D,U</i>	<i>S,U</i>	<i>S,D</i>		
Target	<i>U</i>	<i>S</i>	<i>M</i>	<i>T</i>	<i>T</i>		<i>T</i>	<i>M</i>	<i>S</i>	<i>D</i>	<i>U</i>		
ATT [37]	–	52.8	94.0	85.8	–	–	DCTN [43]	–	70.9	77.5	–	–	
SBA [36]	97.1	50.9	98.4	74.2	87.5	81.6	MM [33]	98.4	72.8	81.3	89.5	96.1	87.6
MALT [28]	97.0	78.7	71.4	98.7	20.7	73.3	OML [24]	98.7	71.7	84.8	91.1	97.8	88.8
MTDA [16]	94.2	52.0	85.5	84.6	91.5	81.5	CMSS [45]	99.0	75.3	88.4	93.7	97.7	90.8
GPLR [29]	89.3	63.4	94.3	97.3	91.8	87.5							
AdaPLR	97.4	61.6	95.4	99.2	99.2	90.6		99.1	95.5	89.6	90.0	97.8	94.4

Table 1: Classification accuracy on Digit5 with a naive 3-layer CNN. Legend: *T*: MNIST, *S*: SVHN, *U*: USPS, *M*: MNIST-*M*, and *D*: Synthetic-Digits.

Source	Multi-Target UDA						Multi-Source UDA						
	<i>P</i>			<i>A</i>			Avg.	<i>C,P,S</i>	<i>A,P,S</i>	<i>A,C,S</i>	<i>A,C,P</i>	Avg.	
	<i>A</i>	<i>C</i>	<i>S</i>	<i>P</i>	<i>C</i>	<i>S</i>		<i>A</i>	<i>C</i>	<i>P</i>	<i>S</i>		
Target	<i>A</i>	<i>C</i>	<i>S</i>	<i>P</i>	<i>C</i>	<i>S</i>		<i>C,P,S</i>	<i>A,P,S</i>	<i>A,C,S</i>	<i>A,C,P</i>		
1-NN*	15.2	18.1	25.6	22.7	19.7	22.7	20.7	DD [27]	87.5	87.0	96.6	71.6	85.7
ADDA*	24.3	20.1	22.4	32.5	17.6	18.9	22.6	SIB [18]	88.9	89.0	98.3	82.2	89.6
DSN*	28.4	21.1	25.6	29.5	25.8	24.6	25.8	OML [24]	87.4	86.1	97.1	78.2	87.2
ITA*	31.4	23.0	28.2	35.7	27.0	28.9	29.0	RABN [42]	86.8	86.5	98.0	71.5	85.7
KD [1]	24.6	32.2	33.8	35.6	46.6	57.5	46.6	JiGen [2]	84.8	81.0	97.9	79.0	85.7
								CMSS [45]	88.6	90.4	96.9	82.0	89.5
AdaPLR	80.1	76.1	25.9	96.0	82.8	49.8	68.4		90.8	89.5	98.8	85.2	91.1

Table 2: Classification accuracy on PACS with ResNet18. * results are taken from [16]. Legend: *A*: Art-Painting, *C*: Cartoon, *P*: Photo, and *S*: Sketch.

Source	Single-Source UDA						Avg.
	<i>P</i>	<i>P</i>	<i>P</i>	<i>A</i>	<i>A</i>	<i>A</i>	
	<i>A</i>	<i>C</i>	<i>S</i>	<i>P</i>	<i>C</i>	<i>S</i>	
Target	<i>A</i>	<i>C</i>	<i>S</i>	<i>P</i>	<i>C</i>	<i>S</i>	
AdaPLR	82.6	80.5	32.3	98.4	84.3	56.1	72.4

Table 3: Classification accuracy on PACS with ResNet18.

enough for the rest. For training the final target model, 100 epochs were sufficient in all the cases.

4.2. Ablation Study

We ablate the design choices described in section 3 on the SVHN→MNIST adaptation task. Parameters found here are then used in all subsequent experiments.

The adaptive property of AdaPLR is a function of α . We consider $N_e = 1$ (*i.e.*, no ensemble) to ablate the different values of α . Figure 6a shows that $\alpha = 0.90$ results in the highest noise reduction, whereas $\alpha = 0.50$ is the least effective. These findings make sense, since with $\alpha = 0.50$, the reassignment would start too early (*i.e.*, as soon as some example has confidence greater than 0.5, since γ is always zero beforehand), when the network is not yet "ready" for it. Instead, with $\alpha = 0.90$, reassignment will start only when some samples have very high confidence. From that moment on, γ starts adapting, so that the more the samples with high confidence, the more permissive the threshold γ will be. The reason $\alpha = 0.95$ results slightly less effective is because a relatively higher number of noisy samples overfits before they are reassigned.

Keeping $N_e = 1$ and $\alpha = 0.9$, we ablate on the different values of parameter N_{RL} (Figure 6b). Results show that $N_{RL} = 3, 4$, or 5 can be considered as the legitimate choice. Further, the results shown in Figure 6c exhibit the

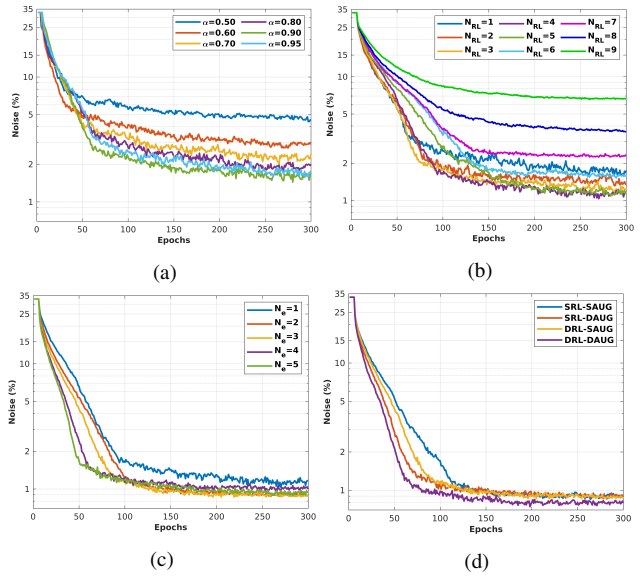


Figure 6: Ablation study considering SVHN→MNIST UDA task to determine optimal parameters of our proposed AdaPLR method. (a): Single model is trained with 1 residual-label (RL) to choose the best α required to compute adaptive noise filtering threshold γ . (b): Searching for the right number of RL *i.e.*, N_{RL} . (c): Searching for the optimal number of members in the ensemble network ($N_{RL} = 4$ is used for $N_e = 1$). (d): Investigating the effect of same/disjoint RL (SRL and/or DRL) and same/different data augmentation (SAUG and/or DAUG) in all four possible scenarios.

improvement achieved by the RL approach in comparison to $N_e = 1$ (with $N_{RL} = 4$, *i.e.* the best choice found in Figure 6b). Though faster noise reduction is achieved with higher number of ensemble members, $N_e = 3$ can be re-

Methods	<i>plane</i>	<i>bcycl</i>	<i>bus</i>	<i>car</i>	<i>horse</i>	<i>knife</i>	<i>mcycl</i>	<i>person</i>	<i>plant</i>	<i>skate</i>	<i>train</i>	<i>truck</i>	Avg.
MCD [38]	87.0	60.9	83.7	64.0	88.9	79.6	84.7	76.9	88.6	40.3	83.0	25.8	71.9
GPDA [20]	83.0	74.3	80.4	66.0	87.6	75.3	83.8	73.1	90.1	57.3	80.2	37.9	73.3
SAFN [44]	93.6	61.3	84.1	70.6	94.1	79.0	91.8	79.6	89.9	55.6	89.0	24.4	76.1
DSBN [3]	94.7	86.7	76.0	72.0	95.2	75.1	87.9	81.3	91.1	68.9	88.3	45.5	80.2
DADA [39]	92.9	74.2	82.5	65.0	90.9	93.8	87.2	74.2	89.9	71.5	86.5	48.7	79.8
AdaPLR	94.5	60.8	92.3	87.3	87.3	93.2	87.6	91.1	56.9	83.4	93.7	86.6	84.2

Table 4: Classification accuracy on Visda-C with ResNet101.

Target	<i>C</i>	<i>I</i>	<i>P</i>	<i>Q</i>	<i>R</i>	<i>S</i>	Avg.
MM [33]	58.6	26.0	52.3	6.3	62.7	49.5	42.6
OML [24]	62.8	21.3	50.5	15.4	64.5	50.4	44.1
CMSS [45]	64.2	28.0	53.6	16.0	63.4	53.8	46.5
AdaPLR	68.3	22.1	54.7	22.8	67.3	57.1	48.7

Table 5: Classification accuracy on DomainNet with ResNet101. For each target, the rest of the domains are considered as source (multi-source UDA). Legend: *C*: Clipart, *I*: Infograph, *P*: Painting, *Q*: Quickdraw, *R*: Real, and *S*: Sketch.

garded as the optimal choice considering performance vs. computational cost trade-off. Such improvement is a consequence of the strong consensus obtained from the ensemble network since $N_e - 1$ members always receive noiseless feedback, while only one member may be partially affected.

Also, as shown in Figure 6d, just one type of augmentation for all the ensemble members (ref. SAUG in the figure) is not enough. Also, the results validate the ineffectiveness of using same residual labels (SRL) for all. The best noise reduction is achieved using Disjoint Residual Labels along with different stochastic augmentations, DRL and DAUG in the figure, respectively (for more details see the Appendix.).

4.3. Results

The reported results in Table 1-5 represent the mean of 3 runs³. In Table 1 (left), we compare AdaPLR with the existing methods which address the challenging $MNIST \rightarrow SVHN$ and $MNIST \rightarrow MNIST-M$ tasks in a multi-target UDA framework. In both cases, the source contains gray-scale images, and the target holds colored (RGB) images, carrying a massive distribution gap across domains for which our method achieves third and second-best performance, respectively. Nevertheless, by outperforming in 3 out of 5 cases, our method achieves state-of-the-art average accuracy. For multi-source UDA task in Table 1 (right), the performance of proposed AdaPLR method is slightly affected while adapting to *Synthetic-Digits* benchmark. However, in the remaining 4 out of 5 cases, our method outperforms existing methods and achieves state-of-the-art average accuracy. Especially, the difference is substantial in the case of $MNIST-M$.

In Table 2 (left), we compare AdaPLR with the existing methods addressing multi-target UDA on PACS. As can be noticed, despite the sub-optimal performance in 2 cases,

³Additional details such as standard deviation and remaining noise in refined pseudo-labels are provided in the Appendix

our method achieves superior average accuracy. For multi-source UDA, we compare recent works in Table 2 (right). Also in this framework, our method consistently outperforms existing methods, with only in one case getting lower, but comparable, accuracy. To the best of our knowledge, we are the first to report single-source UDA results on PACS. So, in Table 3, we consider similar pairs as of Table 2 (left) to evaluate the performance difference. As expected, single-source UDA brings comparatively better performance because of the pair-wise UDA.

In Table 4, along with 2 comparable results for Visda-C, the proposed AdaPLR method achieves superior performance in 6 out of 12 categories that give rise to state-of-the-art average accuracy on such a challenging benchmark. Also In Table 5, except one case, AdaPLR consistently outperforms existing methods despite the large number of classes and discrepancy across domains.

Discussion. In the context of pseudo-label refinery framework, the single-source and multi-target UDA cases can be considered as the most challenging tasks since the pre-trained source model is optimized for one particular data distribution only. Consequently, inferred pseudo-labels are affected by a comparatively higher amount of shift-noise with respect to the multi-source UDA scenario. Thus, in this case, AdaPLR employs a larger amount of epochs for reducing noise and refining pseudo-labels. On the other hand, starting from a better pre-trained source model in multi-source UDA, AdaPLR performs better and faster. Moreover, there is no existing method in the literature that targets all three frameworks (*i.e.*, single-source, multi-target, and multi-source UDA) at a time. To sum up, AdaPLR outperforms existing methods in all scenarios, even without using source data, which highlights the general applicability of the proposed method to cope with challenging tasks of diverse complexity.

5. Conclusions

In this paper, we proposed a novel approach to address source-free UDA, which is cast from the perspective of pseudo-label refinement. To this end, we proposed a novel Ensemble Learning method based on distinct input and feedback by means of Disjoint Residual Labels under the Negative Ensemble Learning framework. Thanks to this new training procedure that allows an extraordinary clean-

ing of the target data labels, which are sufficient enough to train a single target model by a standard supervised learning method. The proposed approach is found to be quite effective in solving challenging UDA tasks without using source data; it does not require any tuning of parameters and can work in single-source, multi-target, and multi-source scenarios indifferently. Results demonstrate the actual goodness of the proposed approach, outperforming the state-of-the-art average performance in all tested benchmarks.

References

- [1] Atif Belal, Madhu Kiran, Jose Dolz, Louis-Antoine Blais-Morin, Eric Granger, et al. Knowledge distillation methods for efficient unsupervised adaptation across multiple domains. *Image and Vision Computing*, page 104096, 2021. [7](#)
- [2] Fabio M Carlucci, Antonio D’Innocente, Silvia Bucci, Barbara Caputo, and Tatiana Tommasi. Domain generalization by solving jigsaw puzzles. In *Proceedings of the IEEE Conference on Computer Vision and Pattern Recognition*, pages 2229–2238, 2019. [7](#)
- [3] Woong-Gi Chang, Tackgeun You, Seonguk Seo, Suha Kwak, and Bohyung Han. Domain-specific batch normalization for unsupervised domain adaptation. In *Proceedings of the IEEE Conference on Computer Vision and Pattern Recognition*, pages 7354–7362, 2019. [2](#), [8](#)
- [4] Chao Chen, Zhihang Fu, Zhihong Chen, Sheng Jin, Zhaowei Cheng, Xinyu Jin, and Xian-Sheng Hua. Homm: Higher-order moment matching for unsupervised domain adaptation. In *AAAI*, 2020. [2](#)
- [5] Chaoqi Chen, Weiping Xie, Wenbing Huang, Yu Rong, Xinghao Ding, Yue Huang, Tingyang Xu, and Junzhou Huang. Progressive feature alignment for unsupervised domain adaptation. In *Proceedings of the IEEE Conference on Computer Vision and Pattern Recognition*, pages 627–636, 2019. [2](#)
- [6] Boris Chidlovskii, Stephane Clinchant, and Gabriela Csuska. Domain adaptation in the absence of source domain data. In *Proceedings of the 22nd ACM SIGKDD International Conference on Knowledge Discovery and Data Mining*, pages 451–460, 2016. [2](#)
- [7] Safa Cicek and Stefano Soatto. Unsupervised domain adaptation via regularized conditional alignment. In *Proceedings of the IEEE International Conference on Computer Vision*, pages 1416–1425, 2019. [2](#)
- [8] Shaveta Dargan, Munish Kumar, Maruthi Rohit Ayyagari, and Gulshan Kumar. A survey of deep learning and its applications: A new paradigm to machine learning. *Archives of Computational Methods in Engineering*, pages 1–22, 2019. [1](#)
- [9] Debasmit Das and C. S. George Lee. Graph matching and pseudo-label guided deep unsupervised domain adaptation. In Věra Kůrková, Yannis Manolopoulos, Barbara Hammer, Lazaros Iliadis, and Ilias Maglogiannis, editors, *Artificial Neural Networks and Machine Learning – ICANN 2018*, pages 342–352, Cham, 2018. Springer International Publishing. [2](#)
- [10] Bruno Klaus de Aquino Afonso and Lilian Berton. Identifying noisy labels with a transductive semi-supervised leave-one-out filter. *Pattern Recognition Letters*, 2020. [3](#)
- [11] John S Denker, WR Gardner, Hans Peter Graf, Donnie Henderson, Richard E Howard, W Hubbard, Lawrence D Jackel, Henry S Baird, and Isabelle Guyon. Neural network recognizer for hand-written zip code digits. In *Advances in neural information processing systems*, pages 323–331, 1989. [6](#)
- [12] Xibin Dong, Zhiwen Yu, Wenming Cao, Yifan Shi, and Qianli Ma. A survey on ensemble learning. *Frontiers of Computer Science*, pages 1–18, 2020. [3](#)
- [13] Yaroslav Ganin and Victor Lempitsky. Unsupervised domain adaptation by backpropagation. In *International conference on machine learning*, pages 1180–1189. PMLR, 2015. [6](#)
- [14] Nuno C. Garcia, Sarah Adel Bargal, Vitaly Ablavsky, Pietro Morerio, Vittorio Murino, and Stan Sclaroff. DMCL: distillation multiple choice learning for multimodal action recognition. *CoRR*, abs/1912.10982, 2019. [3](#)
- [15] Yixiao Ge, Dapeng Chen, and Hongsheng Li. Mutual mean-teaching: Pseudo label refinery for unsupervised domain adaptation on person re-identification. In *International Conference on Learning Representations*, 2020. [2](#)
- [16] Behnam Gholami, Pritish Sahu, Ognjen Rudovic, Konstantinos Bousmalis, and Vladimir Pavlovic. Unsupervised multi-target domain adaptation: An information theoretic approach. *IEEE Transactions on Image Processing*, 29:3993–4002, 2020. [7](#)
- [17] Bo Han, Quanming Yao, Xingrui Yu, Gang Niu, Miao Xu, Weihua Hu, Ivor Tsang, and Masashi Sugiyama. Co-teaching: Robust training of deep neural networks with extremely noisy labels. In *Advances in neural information processing systems*, pages 8527–8537, 2018. [3](#)
- [18] Shell Xu Hu, Pablo Garcia Moreno, Yang Xiao, Xi Shen, Guillaume Obozinski, Neil Lawrence, and Andreas Damianou. Empirical bayes transductive meta-learning with synthetic gradients. In *International Conference on Learning Representations*, 2020. [7](#)
- [19] Xiang Jiang, Qicheng Lao, Stan Matwin, and Mohammad Havaei. Implicit class-conditioned domain alignment for unsupervised domain adaptation. In *International Conference on Machine Learning*, 2020. [2](#)
- [20] Minyoung Kim, Pritish Sahu, Behnam Gholami, and Vladimir Pavlovic. Unsupervised visual domain adaptation: A deep max-margin gaussian process approach. In *Proceedings of the IEEE Conference on Computer Vision and Pattern Recognition*, pages 4380–4390, 2019. [8](#)
- [21] Youngdong Kim, Junho Yim, Juseung Yun, and Junmo Kim. Nlnl: Negative learning for noisy labels. In *Proceedings of the IEEE International Conference on Computer Vision*, pages 101–110, 2019. [3](#), [4](#), [11](#), [12](#)
- [22] Jogendra Nath Kundu, Naveen Venkat, Rahul M V, and R. Venkatesh Babu. Universal source-free domain adaptation. In *Proceedings of the IEEE/CVF Conference on Computer Vision and Pattern Recognition (CVPR)*, June 2020. [2](#)
- [23] Yann LeCun, Léon Bottou, Yoshua Bengio, and Patrick Haffner. Gradient-based learning applied to document recognition. *Proceedings of the IEEE*, 86(11):2278–2324, 1998. [6](#)

- [24] Da Li and Timothy Hospedales. Online meta-learning for multi-source and semi-supervised domain adaptation. In Andrea Vedaldi, Horst Bischof, Thomas Brox, and Jan-Michael Frahm, editors, *Computer Vision – ECCV 2020*, pages 382–403. Cham, 2020. Springer International Publishing. 7, 8
- [25] Da Li, Yongxin Yang, Yi-Zhe Song, and Timothy M Hospedales. Deeper, broader and artier domain generalization. In *Proceedings of the IEEE international conference on computer vision*, pages 5542–5550, 2017. 6
- [26] Rui Li, Qianfen Jiao, Wenming Cao, Hau-San Wong, and Si Wu. Model adaptation: Unsupervised domain adaptation without source data. In *Proceedings of the IEEE/CVF Conference on Computer Vision and Pattern Recognition*, pages 9641–9650, 2020. 2, 3
- [27] Massimiliano Mancini, Lorenzo Porzi, Samuel Rota Bulò, Barbara Caputo, and Elisa Ricci. Boosting domain adaptation by discovering latent domains. In *Proceedings of the IEEE Conference on Computer Vision and Pattern Recognition*, pages 3771–3780, 2018. 7
- [28] Breton Minnehan and Andreas Savakis. Deep domain adaptation with manifold aligned label transfer. *Machine Vision and Applications*, 30(3):473–485, 2019. 2, 7
- [29] Pietro Morerio, Riccardo Volpi, Ruggero Ragonese, and Vittorio Murino. Generative pseudo-label refinement for unsupervised domain adaptation. In *The IEEE Winter Conference on Applications of Computer Vision*, pages 3130–3139, 2020. 2, 3, 7, 11, 12
- [30] Arun Reddy Nelakurthi, Ross Maciejewski, and Jingrui He. Source free domain adaptation using an off-the-shelf classifier. In *2018 IEEE International Conference on Big Data (Big Data)*, pages 140–145. IEEE, 2018. 2
- [31] Yuval Netzer, Tao Wang, Adam Coates, Alessandro Bisacco, Bo Wu, and Andrew Y Ng. Reading digits in natural images with unsupervised feature learning. 2011. 6
- [32] Giorgio Patrini, Alessandro Rozza, Aditya Krishna Menon, Richard Nock, and Lizhen Qu. Making deep neural networks robust to label noise: A loss correction approach. In *Proceedings of the IEEE Conference on Computer Vision and Pattern Recognition*, pages 1944–1952, 2017. 11, 12
- [33] Xingchao Peng, Qinxun Bai, Xide Xia, Zijun Huang, Kate Saenko, and Bo Wang. Moment matching for multi-source domain adaptation. In *Proceedings of the IEEE International Conference on Computer Vision*, pages 1406–1415, 2019. 2, 6, 7, 8
- [34] Xingchao Peng, Ben Usman, Neela Kaushik, Dequan Wang, Judy Hoffman, and Kate Saenko. Visda: A synthetic-to-real benchmark for visual domain adaptation. In *Proceedings of the IEEE Conference on Computer Vision and Pattern Recognition Workshops*, pages 2021–2026, 2018. 6
- [35] Subhankar Roy, Aliaksandr Siarohin, Enver Sangineto, Samuel Rota Bulò, Nicu Sebe, and Elisa Ricci. Unsupervised domain adaptation using feature-whitening and consensus loss. In *Proceedings of the IEEE Conference on Computer Vision and Pattern Recognition*, pages 9471–9480, 2019. 2
- [36] Paolo Russo, Fabio M Carlucci, Tatiana Tommasi, and Barbara Caputo. From source to target and back: symmetric bi-directional adaptive gan. In *Proceedings of the IEEE Conference on Computer Vision and Pattern Recognition*, pages 8099–8108, 2018. 7
- [37] Kuniaki Saito, Yoshitaka Ushiku, and Tatsuya Harada. Asymmetric tri-training for unsupervised domain adaptation. In *International Conference on Machine Learning*, pages 2988–2997. PMLR, 2017. 7
- [38] Kuniaki Saito, Kohei Watanabe, Yoshitaka Ushiku, and Tatsuya Harada. Maximum classifier discrepancy for unsupervised domain adaptation. In *Proceedings of the IEEE Conference on Computer Vision and Pattern Recognition*, pages 3723–3732, 2018. 8
- [39] Hui Tang and Kui Jia. Discriminative adversarial domain adaptation. In *AAAI*, pages 5940–5947, 2020. 2, 8
- [40] Antonio Torralba and Alexei A Efros. Unbiased look at dataset bias. In *Proceedings of the IEEE/CVF Conference on Computer Vision and Pattern Recognition*, pages 1521–1528, 2011. 1, 4
- [41] Jun Wen, Nenggan Zheng, Junsong Yuan, Zhefeng Gong, and Changyou Chen. Bayesian uncertainty matching for unsupervised domain adaptation. In *Proceedings of the Twenty-Eighth International Joint Conference on Artificial Intelligence, IJCAI-19*, pages 3849–3855. International Joint Conferences on Artificial Intelligence Organization, 7 2019. 2
- [42] Jiaolong Xu, Liang Xiao, and Antonio M López. Self-supervised domain adaptation for computer vision tasks. *IEEE Access*, 7:156694–156706, 2019. 7
- [43] Ruijia Xu, Ziliang Chen, Wangmeng Zuo, Junjie Yan, and Liang Lin. Deep cocktail network: Multi-source unsupervised domain adaptation with category shift. In *Proceedings of the IEEE Conference on Computer Vision and Pattern Recognition*, pages 3964–3973, 2018. 7
- [44] Ruijia Xu, Guanbin Li, Jihan Yang, and Liang Lin. Larger norm more transferable: An adaptive feature norm approach for unsupervised domain adaptation. In *Proceedings of the IEEE International Conference on Computer Vision*, pages 1426–1435, 2019. 8
- [45] Luyu Yang, Yogesh Balaji, Ser-Nam Lim, and Abhinav Shrivastava. Curriculum manager for source selection in multi-source domain adaptation. In *Proceedings of the European Conference on Computer Vision (ECCV)*, 2020. 7, 8
- [46] Xu-Cheng Yin, Kaizhu Huang, Hong-Wei Hao, Khalid Iqbal, and Zhi-Bin Wang. A novel classifier ensemble method with sparsity and diversity. *Neurocomputing*, 134:214–221, 2014. 3
- [47] Zizhao Zhang, Han Zhang, Sercan O Arik, Honglak Lee, and Tomas Pfister. Distilling effective supervision from severe label noise. In *Proceedings of the IEEE/CVF Conference on Computer Vision and Pattern Recognition*, pages 9294–9303, 2020. 3
- [48] Zhi-Hua Zhou. *Ensemble methods: foundations and algorithms*. CRC press, 2012. 3

Appendix

As mentioned in the main paper, the following sections include: (1) Details on the distribution of shift-noise and its impact on negative learning. (2) Noise cleaning performance of the proposed method, together with standard deviations for the final accuracy (not included in the main paper due to lack of space).

On the impact of noise distribution on Negative Learning

Negative Learning (NL) is an indirect learning method in which a model is optimized to produce the lowest confidence to a randomly chosen complementary label for the given input image. Such a method produces more reliable performance in the case of a noisy label set. Nevertheless, the applicability of the existing NL method [21] is limited to a type of noise showing uniform distribution (*Symmetric-Noise*). In order to highlight specific limitations of the existing NL method, figure 7 shows the confusion matrix for the initial noise along with the histograms of the noisy and clean sample’s confidence distribution obtained after training for SVHN \rightarrow MNIST UDA.

As shown in Figure 7a, when labels are initially affected by *Symmetric-Noise*, noisy samples are classified with low confidence whereas the clean samples are leaned to high confidence. Consequently, effective noise separation is achieved.

For the *Asymmetric-Noise*, mimicking some of the structures of real errors [32] *i.e.*, for MNIST, mapping 2 \rightarrow 7, 3 \rightarrow 8, 7 \rightarrow 1, and 5 \leftrightarrow 6, existing NL method’s effectiveness degrades considerably. As can be seen in Figure 7b, noisy samples are overfitted with quite high confidence (even higher than 50%). Yet, sub-optimal separation still exists if we consider only samples carrying confidence higher than 90% (though it is not generalizable for other benchmarks where all clean samples do not carry such high confidence).

Nevertheless, noisy samples are overfitted with very high confidence when *shift-noise* associated with inferred pseudo-labels [29] is considered (Figure 7c). Consequently, subsequent Positive Learning achieves sub-optimal performance with such noise distribution in the UDA framework.

Please note that in all cases, the *amount* of noise is same *i.e.* 32.97%, similar to the amount of shift-noise observed in the case of SVHN \rightarrow MNIST UDA task in Table 6.

Noise Cleaning Performance of AdaPLR

We demonstrate here the adaptive noise filtering and progressive pseudo-label refinement performance of the proposed AdaPLR method. In Figure 8 we evaluate the robustness of our method in achieving effective pseudo-label refinement over three runs while considering the most challenging UDA task *i.e.*, multi-source UDA on DomainNet.

Specifically, Figure 8a shows the adaptiveness of γ threshold for different UDA tasks in which inferred pseudo-labels are affected by the various amount of noise *i.e.*, starting from 31.47% up to 82.40% of shift-noise. As can be seen in Figure 8b, in each case, AdaPLR achieves quite reasonable noise reduction throughout the training process. Such a trend is also observed in single-source UDA on *Digit5* benchmarks (see main paper). However, the only difference in the two cases is that the change in γ threshold is comparatively smoother for *Digit5* which eventually takes more epochs for pseudo-label refinement (and achieves better noise reduction too).

To conclude, in Table 6-9, we summarize statistics concerning classification accuracy along with standard deviations of *inferred* pseudo-labels — obtained using pre-trained source model, *refined* pseudo-labels — obtained using the proposed Negative Ensemble Learning (NEL) technique, and the single-target model trained with the refined pseudo-labels — the final stage of the proposed *AdaPLR* method. In many cases, we achieve better performance with NEL only. However, for a fair comparison with existing works, the main paper compares the results achieved using a single target model only. Yet, the reported results validate that the proposed AdaPLR is remarkably effective and stable for all the UDA benchmarks.

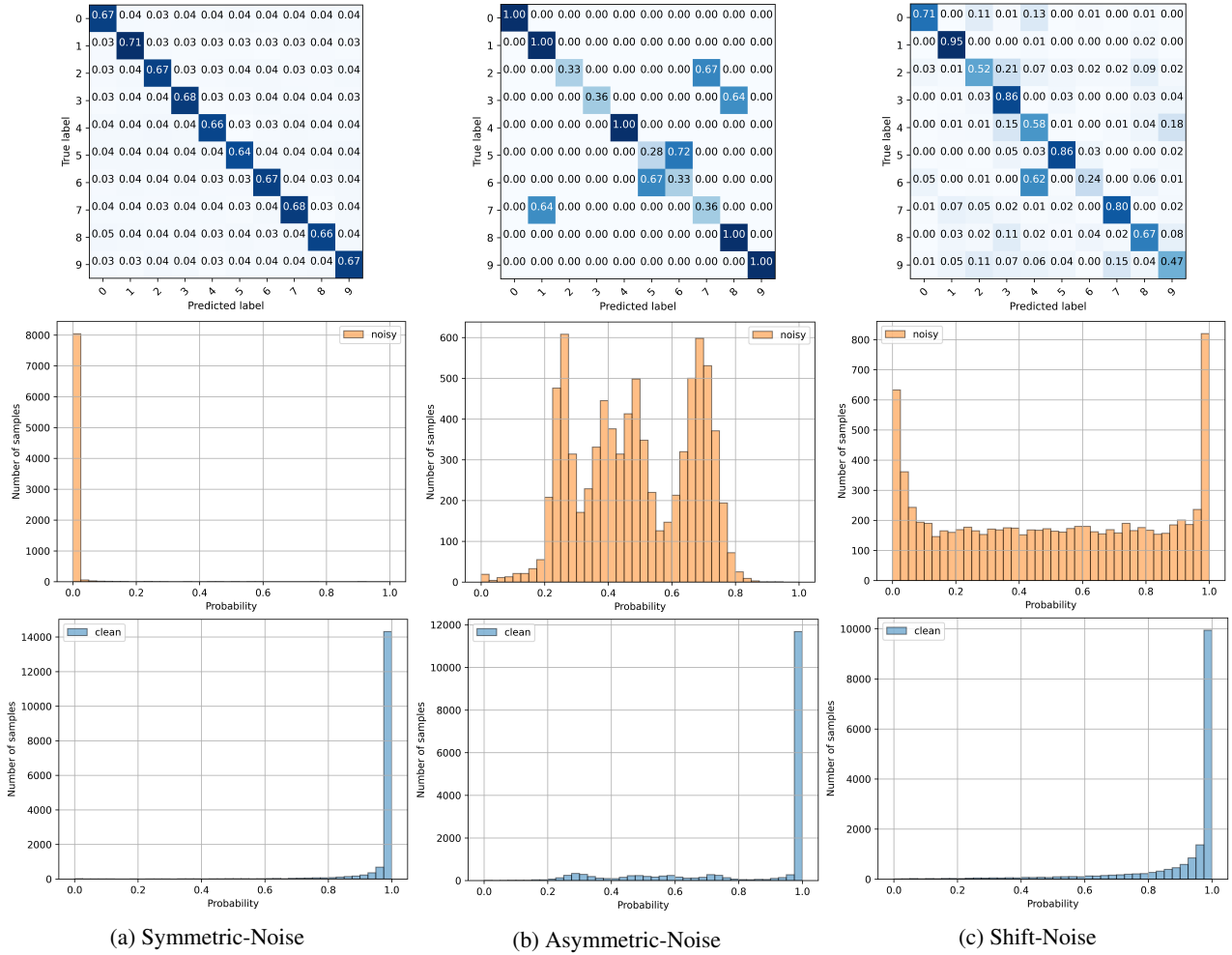


Figure 7: Noise filtering capability of the existing Negative Learning method [21] over various noise distributions. Column (a) Symmetric Noise, column (b) Asymmetric artificial noise [32], column (c) Shift noise [29]. First row: the confusion matrix shows how the noise is distributed in the beginning. Second row: confidence prediction for the noisy samples after training with NL. Third row: confidence prediction for the clean samples after training with NL. The amount of initial noise is same in magnitude (*i.e.* 32.97%) for all the cases.

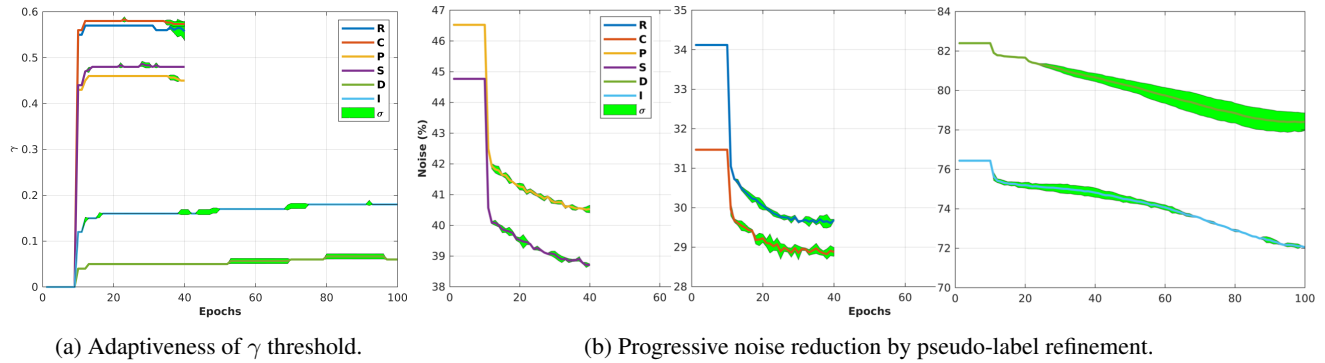


Figure 8: Training evolution on DomainNet. Multi-source case: for each target, the rest of the domains are considered as source. For better representation, we concatenate noise reduction trends with different scales in (b). Legend: *C*: Clipart, *I*: Infograph, *P*: Painting, *Q*: Quickdraw, *R*: Real, *S*: Sketch, and σ : Instantaneous standard deviation of three runs.

Source	<i>T</i>	<i>T</i>	<i>T</i>	<i>S</i>	<i>U</i>	Avg.
Target	<i>U</i>	<i>S</i>	<i>M</i>	<i>T</i>	<i>T</i>	
Inferred	86.3	34.7	63.8	67.0	70.2	64.4
Refined	99.1±0.04	62.0±0.10	97.5±0.03	99.2±0.05	99.2±0.02	91.4±0.05
AdaPLR	97.4±0.10	61.6±0.29	95.4±0.16	99.2±0.02	99.2±0.02	90.6±0.12

(a) Single-Source UDA.

Source	<i>M,S,D,U</i>	<i>T,S,D,U</i>	<i>T,M,D,U</i>	<i>T,M,S,U</i>	<i>T,M,S,D</i>	Avg.
Target	<i>T</i>	<i>M</i>	<i>S</i>	<i>D</i>	<i>U</i>	
Inferred	98.6	69.1	52.0	40.3	88.7	69.8
Refined	98.8±0.95	94.2±0.18	84.6±0.66	87.8±0.85	98.6±0.03	92.8±0.53
AdaPLR	99.1±0.02	95.5±0.71	89.6±0.55	90.0±0.63	97.8±0.15	94.4±0.41

(b) Multi-Source UDA.

Table 6: Results on Digit5. Legend: *T*: MNIST, *S*: SVHN, *U*: USPS, *M*: MNIST-M, and *D*: Synthetic-Digits.

Source	<i>P</i>			<i>A</i>			Avg.
Target (Combined)	<i>A,C,S</i>			<i>P,C,S</i>			
Inferred	37.7			57.9			47.8
Refined	57.3±1.13			73.8±0.81			65.6±0.97
Target	<i>A</i>	<i>C</i>	<i>S</i>	<i>P</i>	<i>C</i>	<i>S</i>	Avg.
AdaPLR	80.1±0.37	76.1±1.62	25.9±0.82	96.0±0.34	82.8±1.09	49.8±0.89	

(a) Multi-Target UDA. The final accuracy on each target is achieved using the same target model trained with refined pseudo-labels.

Source	<i>P</i>	<i>P</i>	<i>P</i>	<i>A</i>	<i>A</i>	<i>A</i>	Avg.
Target	<i>A</i>	<i>C</i>	<i>S</i>	<i>P</i>	<i>C</i>	<i>S</i>	
Inferred	60.9	24.8	26.5	96.0	58.1	43.9	51.7
Refined	81.1±0.44	76.9±1.36	31.7±0.98	98.2±0.19	80.9±0.77	51.2±1.04	70.0±0.80
AdaPLR	82.6±0.83	80.5±2.66	32.3±0.68	98.4±0.03	84.3±1.50	56.1±1.27	72.4±1.16

(b) Single-Source UDA.

Source	<i>C,P,S</i>	<i>A,P,S</i>	<i>A,C,S</i>	<i>A,C,P</i>	Avg.
Target	<i>A</i>	<i>C</i>	<i>P</i>	<i>S</i>	
Inferred	78.4	77.9	95.3	64.5	79.0
Refined	89.3±0.36	87.2±0.15	98.1±0.23	83.2±0.86	89.5±0.40
AdaPLR	90.8±0.08	89.5±0.54	98.8±0.12	85.2±0.73	91.1±0.37

(c) Multi-Source UDA.

Table 7: Results on PACS. Legend: *A*: Art-Painting, *C*: Cartoon, *P*: Photo, and *S*: Sketch.

Methods	<i>plane</i>	<i>bycycl</i>	<i>bus</i>	<i>car</i>	<i>horse</i>	<i>knife</i>	<i>mcycl</i>	<i>person</i>	<i>plant</i>	<i>skate</i>	<i>train</i>	<i>truck</i>	Avg.
Inferred	64.2	6.3	75.2	21.7	55.9	95.7	22.8	1.4	79.8	0.7	82.8	19.8	46.3
Refined	95.2	64.8	90.8	89.7	87.4	93.7	91.5	88.5	56.4	82.9	97.1	93.8	85.1
AdaPLR	±0.05	±0.11	±0.23	±0.27	±0.08	±0.51	±0.21	±0.66	±1.01	±0.37	±0.09	±0.15	±0.31
	94.5	60.8	92.3	87.3	87.3	93.2	87.6	91.1	56.9	83.4	93.7	86.6	84.2
	±0.29	±0.31	±0.46	±0.78	±0.55	±0.02	±0.58	±0.27	±0.09	±0.44	±0.07	±0.74	±0.38

Table 8: Results on Visda-C.

Target	<i>C</i>	<i>I</i>	<i>P</i>	<i>Q</i>	<i>R</i>	<i>S</i>	Avg.
Inferred	68.5	23.6	53.5	17.6	65.9	55.2	47.4
Refined	71.1±0.11	28.0±0.05	59.5±0.12	21.6±0.44	70.4±0.04	61.3±0.03	52.0±0.13
AdaPLR	68.3±0.15	22.1±0.17	54.7±0.15	22.8±0.45	67.3±0.92	57.1±0.27	48.7±0.35

Table 9: Multi-Source UDA results on DomainNet. Legend: *C*: Clipart, *I*: Infograph, *P*: Painting, *Q*: Quickdraw, *R*: Real, and *S*: Sketch.